

# HEMT's Design for Applications beyond 100GHz

S. Bollaert, T. Parenty, X. Wallart, H. Happy, G. Dambrine, A. Cappy

Institut d'Electronique, de Microelectronique et de Nanotechnologies

UMR CNRS 8520

Département Hyperfréquences & Semiconducteurs

Cité Scientifique, Avenue Poincaré, BP 69

59652 Villeneuve d'Ascq Cedex

France

sylvain.bollaert@iemn.univ-lille1.fr

## I. Introduction

Electronics up to 100 GHz have applications in atmospheric sensing, radio astronomy, passive imaging applications, wide-band communication systems. Millimeter Wave (MMW) analog and numerical circuits have to be developed. HEMTs on InP substrate are largely used in D-band (110-150 GHz) [1-5] and G-band (140-220GHz) [6-8] circuits. Improvement of frequency operation has been obtained by reduction of gate length to nanometer values [6-7] and higher Indium content up to 80%. Another field of application is induced by the demand of higher bit-rate communication, which is rapidly growing. 40Gbit/s system has been recently developed [9] and intensive research on 80Gbit/s and 160Gbit/s is being done. Analog and numerical circuits used in such optical transmission systems can also be realized with nanometer gate length InP-based HEMTs [10-11]. With InP-based HEMTs, it is possible to reach  $f_T$  higher than 472GHz [11] with 30 nanometer gate length. To obtain that good value, gate recess undercut has been optimized.

Cutoff frequency  $f_T$  is an important parameter in particularly for numerical circuits. However reduction of gate length will involve an increase of short channel effects. This point will limit the maximum oscillation frequency  $f_{max}$  and microwave performance of analog circuits. To avoid this effect, layer structure has to be correctly designed for sub-100 nanometer gate length HEMTs. In this paper, we present an optimized InAlAs/InGaAs/InP layer structure for sub-100 nanometer gate length HEMTs using a scaling down rule. HEMTs have been fabricated on such layer structure and compared with devices fabricated on standard structure usually used for 100 nanometer gate length HEMTs. Same gate lithography of 70 nanometer length has been achieved on both layer structures. DC and microwave characteristics are compared. Degradation of  $f_{max}$  in short channel HEMTs can be overcome by the use of transferred-substrate technological process. This technique offers the possibility to realize insulating buffer HEMTs or by the addition of a second gate under the channel, (double gate HEMTs). Technological process and electrical results of TS-HEMTs will be presented in this paper. Finally passive elements and specially transmission lines will be described and presented. These elements are also a limiting factor for the frequency raise of mm-wave circuits. Indeed these passive structures have to present low loss, high characteristic impedance range. Moreover for high speed mixed-mode circuits, these transmission lines have to be blinded to avoid any clock cross-talk phenomena.

## II. Design and realization of sub 100nm gate length HEMTs

The increase of the HEMTs performance is possible with obviously the reduction of the gate length, but it's not enough to achieve the best results. The aspect ratio defined as the gate length  $L_g$  over the gate-to-channel distance  $A$  has to be kept high enough to avoid short channel effects. It is important to find a good trade-off between a high aspect ratio and several physical limitations as the tunneling current across the Schottky barrier, the increase of the quantum energy levels in the quantum well, or the loss of mobility with the reduction of the spacer layer.

On the figure 1.a), we present the standard layer structure currently used for 100 nm gate length HEMTs. In this structure the aspect ratio  $L_g/A$  is close to 6 for a 100 nm gate length. For a 50 nm gate length, this value is only 3. To keep a constant value for the 50 nm gate length and so avoid short channel effects, the distance of gate-to-channel  $A$  has to be reduced. On figure 1.b), we show the optimized layer structure for 50 nm gate length HEMTs. The gate-to-channel distance can not be further reduced, because of gate tunneling current and depletion from the surface of the carrier in the

channel near the recessed region. To improve Schottky characteristics and the confinement of electrons in the channel, aluminum content in the InAlAs layers has been fixed to a higher value of 0.65. In the channel, we choose an indium content of 0.65 to improve carrier transport properties. Moreover, to avoid degradation due to the depletion of channel induced by the surface states in the recess, we raised the  $\delta$ -doping at  $6 \times 10^{12} \text{ cm}^{-2}$  for the optimized structure (figure 1.b). To limit parasitic effects, as tunneling current or parasitic conduction in the  $\delta$ -doping layer, the  $\delta$ -doping cannot be increased to higher value. Monte-Carlo simulation has been used to confirm choices on this new layer structure. Details and results of simulations are given elsewhere [12].

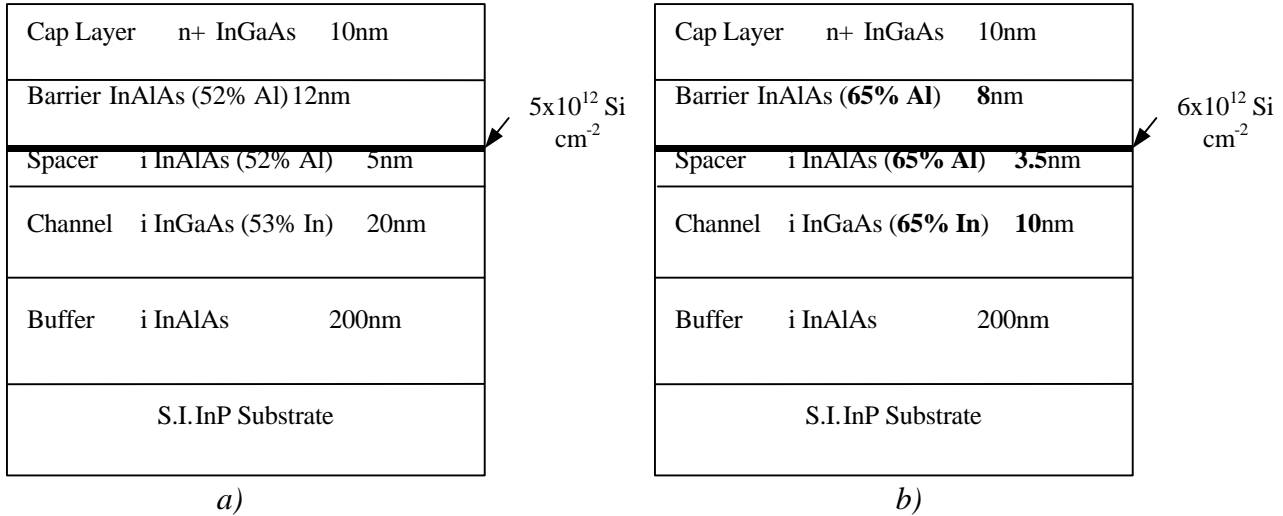


Figure 1 : Standard (a) and optimized (b) layer structures.

Standard and optimized structures were realized by molecular beam epitaxy. 70 nm gate length HEMTs with same technological process were fabricated on the standard (figure 1.a) and the optimized (figure 1.b) structures. First the mesa isolation was defined by  $\text{H}_3\text{PO}_4:\text{H}_2\text{O}_2:\text{H}_2\text{O}$  solution. Ohmic contact Ni/Ge/Au/Ni/Au was evaporated followed by 1 minute rapid thermal annealing at 310 °C. Typical ohmic contact resistance of 0.15 to 0.2  $\Omega \cdot \text{mm}$  was measured. The T-shaped gate was defined by electron beam lithography. InGaAs cap layer was selectively removed using succinic acid, ammonia and hydrogen peroxide mixture. Finally Ti/Pt/Au gate was evaporated as well as the bonding pads.

DC characteristics of a 70-nm-gate HEMT on the new layer structure exhibit a maximum transconductance  $g_m$  about 1 S/mm. Pinch-off voltage  $V_p$  is  $-0.4$  V. Drain-to-source current  $I_{ds}$  reaches a value of 560 mA/mm. For the standard structure,  $V_p$  is  $-0.7$  V and  $I_{ds}$  is 500 mA/mm. The DC-transconductance is about 750 mS/mm.

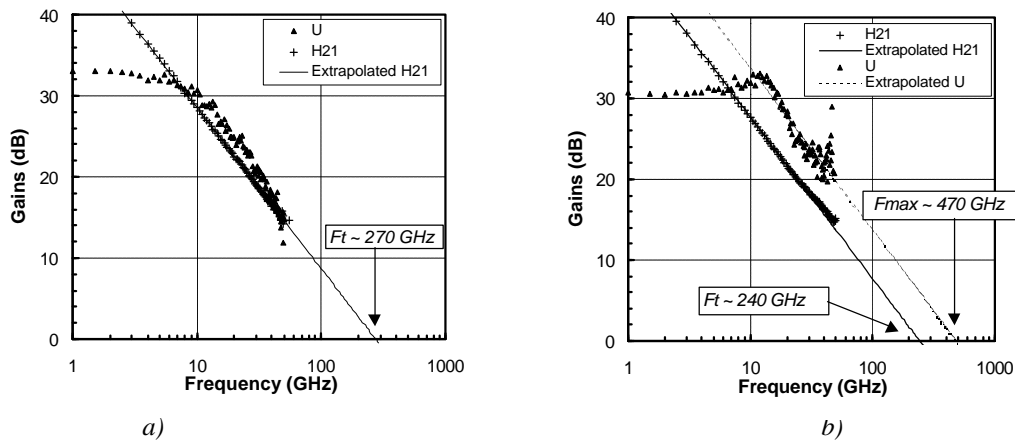


Figure 2 : Performances of 60nm x 100µm HEMT processed on a standard (a) and optimized (b) layer structures .

On-Wafer S-parameters measurements were performed up to 50GHz for both devices. Small signal equivalent circuit has been extracted. On the intrinsic transconductance, a large improvement is

obtained with the optimized structure. Values for the standard HEMTs and the optimized HEMTs are respectively 1180 and 1550 mS/mm. That difference confirms the improvement of the aspect ratio  $L_g/A$  of the optimized structure. Figure 2 shows the extrinsic  $|H_{21}|^2$  and unilateral gain  $U$  versus frequency for the 70nm-HEMTs realized on a standard (a) and optimized (b) layer structure.  $f_T$  of the HEMT on the optimized structure is 240GHz. For the standard LM-HEMT, we obtained a  $f_T$  of 270 GHz. The maximum oscillation frequency  $f_{max}$  for the optimized HEMT is 470 GHz, and exceeds largely the 260 GHz value obtained with the standard structure. This high  $f_{max}$  is related to the improved ratios  $g_m/g_d$  and  $C_{gs}/C_{gd}$  (intrinsic values) obtained with the optimized layer (respectively 18.7 and 7.8) in comparison with the standard layer (respectively 6.7 and 5.1). This is due to a reduction of short channel effects and improvement of charge control.

### III. Transferred Substrate HEMTs

In sub-0.1  $\mu\text{m}$  gate length device, short-channel effect will be a limiting factor in the improvement of  $f_{max}$ . Indeed injection of carriers in the substrate, when shorting gate length, will drastically degrade the output conductance  $g_d$  of the device. The way to suppress injection of these carriers is to replace the substrate by an insulating layer. This can be achieved by a transferred-substrate technique previously used in SOI-MOS and TS-HBT technologies [13].

Lattice-matched InAlAs/InGaAs layers were grown on 2-inch InP substrate by Molecular Beam Epitaxy. In comparison to typical structure used for conventional lattice-matched HEMTs on InP substrate, the heterostructure has been reverse grown. The main difficulty associated with the growth of the reverse heterostructure is the Silicon segregation from the cap layer in the Schottky contact layer and more from the delta-doping plane in the channel layer which drastically reduces the electron mobility. These have been overcome by choosing a suitable growth temperature sequence.

Figure 3 shows the schematic cross section the InAlAs/InGaAs/InP structure transferred on the Silicon substrate. InAlAs/InGaAs/InP HEMTs structure and Silicon wafer were bonded by means of  $\text{SiO}_2\text{-SiO}_2$  bonding (Thickness  $\sim 550$  nm). 2-inch wafer bonding has been processed at CEA-LETI [14]. Fabrication of HEMTs requires InP substrate and etch-stop layers removing, to uncover the cap layer. At this step of the process, Hall measurement has been achieved at room temperature, to verify growth quality and influence of bonding. The sheet carrier density and Hall mobility are respectively  $3.2 \cdot 10^{12} / \text{cm}^2$  and  $6900 \text{ cm}^2/\text{Vs}$ . These values are weakly affected by the reverse epitaxial growth, compared with typical values obtained with conventional heterostructure used for LM-HEMTs. Then the  $0.12 \mu\text{m}$  T-shaped gate length HEMT fabrication can be started. It is exactly the same process used on classical LM-HEMTs, reported before.

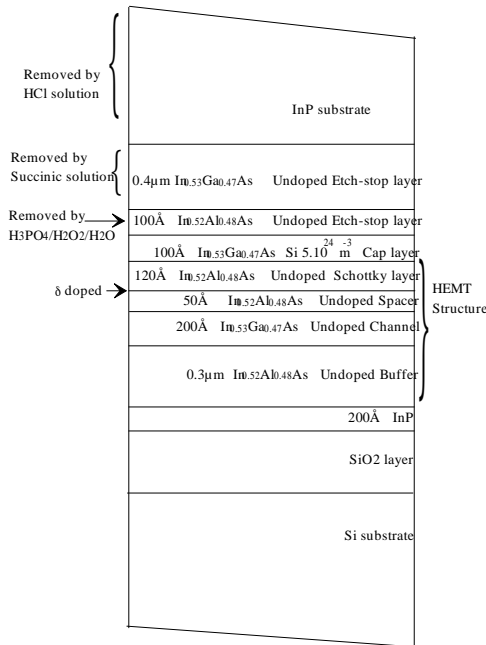


Figure 3 Cross section of HEMTs structure reported on Silicon substrate by  $\text{SiO}_2\text{-SiO}_2$  bonding.

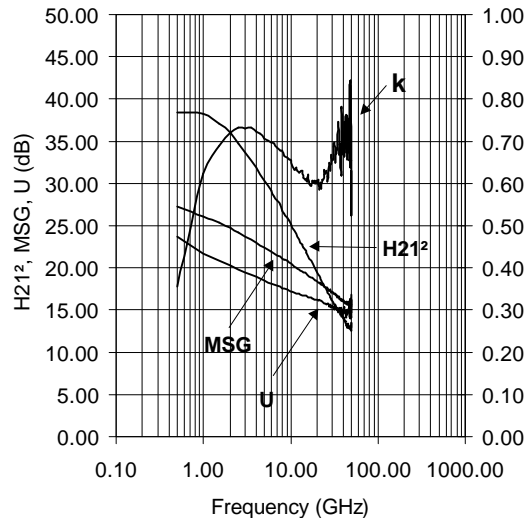


Figure 4 Microwave gains of  $0.12 \mu\text{m}$  transferred-substrate HEMTs.

DC and microwave characteristics of 100  $\mu\text{m}$  wide TS-HEMTs were measured on wafer. The device exhibits maximum drain-to-source current  $I_{\text{ds}} = 450 \text{ mA/mm}$ . The maximum extrinsic transconductance  $g_m$  is 770mS/mm. Using S-parameters measurement in the 0-50GHz frequency range, calculated extrinsic current gain  $|H_{21}|^2$ , maximum stable gain MSG and unilateral gain U are plotted in figure 4 versus frequency. Extrapolation by 20 dB/decade of  $|H_{21}|^2$  gives an extrinsic cutoff frequency  $f_T$  of 185 GHz. This result is close to published results obtained with LM-HEMT on InP [15]. Maximum oscillation frequency  $f_{\text{max}}$  deduced from extrapolation by 20 dB/decade of U is 280 GHz. This evidences the growth quality of the reverse heterostructure and shows that the transferred-substrate process affects very weakly the microwave performances of the TS-HEMTs.

## References

- [1] S. Weinreb et al, "Full-waveguide band 90 to 140 GHz, MMIC amplifier module", IEEE MTT-S Digest 1997, pp.1279-1280
- [2] C. Probanz et al, "A High-Gain Monolithic D-band InP HEMT Amplifier", GaAs IC 98, pp. 41-44
- [3] H. Wang et al, "A 155-GHz Monolithic Low-Noise Amplifier", IEEE Trans. On Microwave Theory and Techniques, vol. 46, NO. 11, pp.1660-1666, NOVEMBER 1998
- [4] D.L. Edgar et al, "94 and 150GHz coplanar waveguide MMIC amplifiers realized using InP technology", IEEE MTT-S Digest 1999.
- [5] M. Nishimoto et al, "High performance D-band (118 GHz) monolithic low-noise amplifier", IEEE MTT-S Digest 1999
- [6] R. Lai et al, "InP HEMT Amplifier Development for g-band (140-220 GHz) Applications", IEDM 2000
- [7] C. Pobanz et al, "High Performance MMICs with Submillimeter Wave InP-based HEMTs", IPRM 2000, pp. 67-70
- [8] R. Raja et al, "A 183 GHz low noise amplifier module with 5.5 dB noise figure for the conical-scanning microwave imager sounder (CMIS) program", IEEE MTT-S Digest 2001
- [9] T. Enoki, Y. Ishii, "InP-Based HEMT Technologies for High-Speed ICs", URSI' 99.
- [10] D. Xu et al, "Depletion and enhancement mode modulation field effect transistor for ultra-high speed applications: an electrochemical fabrication technology", IEEE transactions on electron devices, vol.47, n°1, January 2000.
- [11] K. Shinohara et al, "Importance of gate recess structure to the cutoff frequency of ultra-high-speed InGaAs/InAlAs HEMTs", IPRM2002, pp.451-454.
- [12] J. Mateos et al, "Design Optimisation of Ultra-Short Gate HEMTs Using Monte Carlo Simulation" GAAS 2000, pp.624-627.
- [13] M. Urtega et al, "185 GHz Monolithic Amplifier in InGaAs/InAlAs Transferred-Substrate HBT Technology", IEEE MTT-S Digest 2001
- [14] S. Bollaert et al, "0.12 $\mu\text{m}$  Transferred-Substrate InAlAs/InGaAs HEMTs on Silicon Wafer", IEEE Electron Device Letters, vol. 25, n°2, February 2002.
- [15] L. D. Nguyen et al, "Ultra-high speed modulation doped field effect transistor: a tutorial review", Proceeding of the IEEE, vol. 80, n°4, April 1992, pp. 494-518.